geoconvention
Calgary • Canada • May 13-17 2019

Empirical and numerical investigation of the effects of in situ stress regime on induced seismicity magnitude distribution

Ali Mehrabifard[1], Erik Eberhardt[1], Branko Damjanac [2]*

[1] Geological Engineering, University of British Columbia, Vancouver, BC, Canada

[2] Itasca Consulting Group, Inc., Minneapolis, MN, USA

Summary

Empirical data has been compiled of recorded seismic data for several different shale gas basins in North America, with particular focus on the Montney in British Columbia and the Woodford in Oklahoma. By applying temporal and spatial filters to well activity, induced seismicity related to hydraulic fracturing activities (both hydraulic fracturing and waste water injection) have been identified. The stress regimes were determined based on the reported focal mechanisms of the induced seismic events. The data was then analyzed using the Gutenberg-Richter relationship for the magnitude-frequency distribution of the identified induced seismic events. From this, the 'b-value' for the Montney and Woodford shale basins were determined. The comparison between the interpreted stress regime (from focal mechanisms) and the relevant estimated b-values reveals that the thrust faulting regime that is more dominant in the Montney has a lower b-value than the strike-slip regime that is more dominant in the Woodford. Accordingly, it was found that the potential for larger magnitude earthquakes is higher in a thrust faulting regime. This finding and the mechanistic cause for it was further investigated using a new 3-D hybrid lattice and particle-bonded code XSite™ (Damjanac at al., 2016). The simulation results from the modelling investigation are compared with the results from the empirical analysis and provide mechanistic insights relative to other fault characteristics such as sensitivity to fault angle and strength.

Theory and Methodology

Hydraulic fracturing techniques have evolved over the last 50 years, from a means to stimulate conventional oil and gas reservoirs to playing an essential role, via multi-stage hydraulic fracturing and extended-reach horizontal wellbores, in making unconventional reservoirs economically viable. However, this development has been accompanied by growing public, industry, and regulator concerns regarding induced seismicity (Bunger et al., 2013; Cipolla et al., 2008; Maxwell, 2013; Rutqvist et al., 2013). Fluid injection in deep wells, either during hydraulic fracturing treatments or subsequent waste water disposal, acts to increase the formation pore pressures, which in turn can decrease the effective normal stresses acting on a fault. This reduces the resistance to shear along the fault, triggering slip and releasing the stored strain energy (Healy et al., 1968). Consequently, the stress regime (e.g., thrust, strike-slip, normal, etc.) represents an important boundary condition; the fault characteristics (e.g., orientation, continuity, structural complexity) controls the available shear strength and strain energy stored; and the operational factors (e.g., injection volume, rate, etc.) act as a triggering source. Each can be considered to be a key parameter that influences the induced seismicity magnitude and affects the magnitude distribution. In this paper, several of these effects with particular focus on the influence of different stress regimes have been investigated by integrating an empirical study of recorded seismic events for different North American shale gas basins with advanced 3-D numerical modelling.

Analysis, Discussion and Key Findings

A database of the focal mechanisms related to induced seismicity measured in the Montney and Woodford was prepared to correlate the distribution of event magnitudes to the tectonic stress regime prevalent for each shale basin (Figure 1 and 2). Using the Gutenberg-Richter relationship (Gutenberg & Richter, 1944) for magnitude-frequency distribution of the identified induced seismic events, the 'b-values' were calculated for each shale basin using the maximum likelihood method (Aki, 1965; Utsu, 1965). The magnitude of completeness was estimated using the maximum curvature method suggested by Wiemer and Wyss (2000). By comparing the calculated 'b-values' for different stress regimes (Figure 3), one could conclude that thrust faulting regimes have a higher potential for larger magnitude induced seismicity events as indicated by its lower b-value than those associated with a strike-slip regime. This observation is consistent with previous observations of the correlation between b-value and different stress regimes in both tectonic earthquakes (Scholz, 2015; Schorlemmer et al., 2005) and laboratory tests (Goebel et al., 2017).

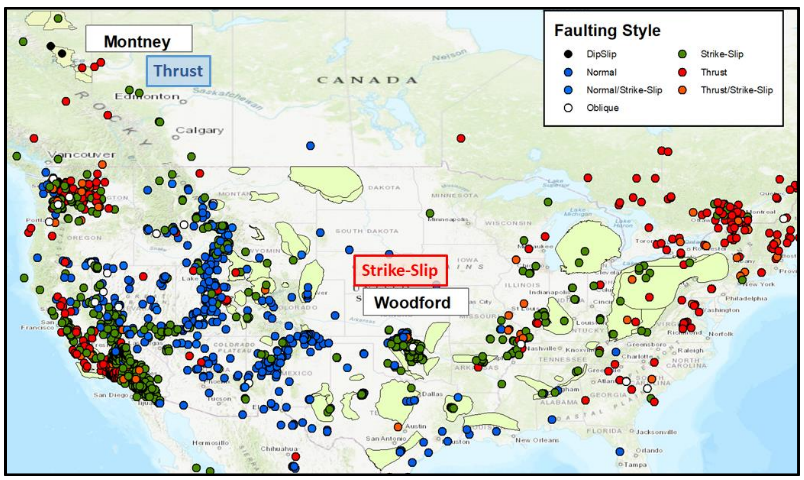

Figure 1 - Focal mechanism and shale basins, after (Amini & Eberhardt, 2017)

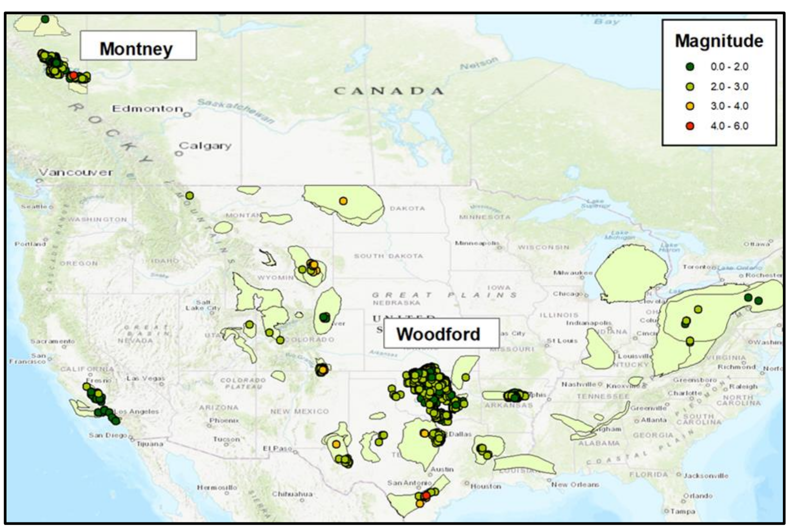

Figure 2 - Identified induced seismic events and their magnitudes (Amini & Eberhardt, 2017)

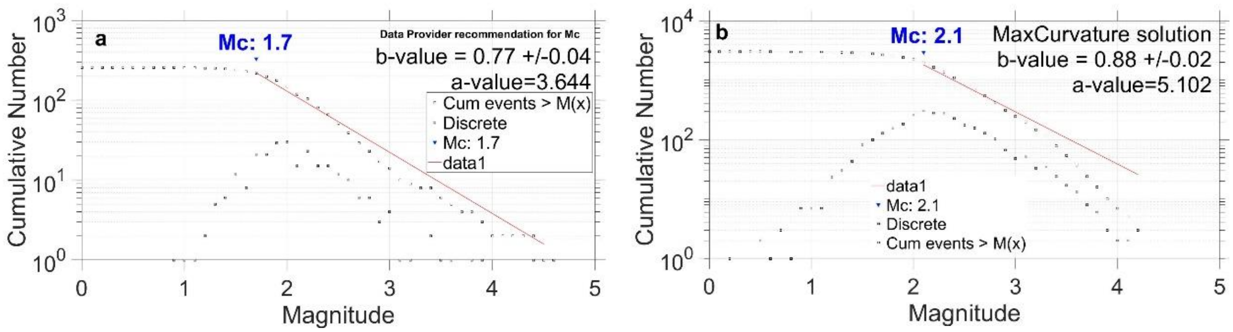

Figure 3 - Magnitude distribution and b-values in the: a) Montney, and b) Woodford

Additive information to investigate the mechanistic reasons for this result was provided through advanced numerical modelling. A key step before conducting any numerical analyses is selecting the most appropriate technique; each method has its own advantages and limitations and these need to be weighed against the questions the model is intended to address. For the case of hydraulic fracturing and fault slip, continuum methods (e.g., FEM) are limited in how they can represent the presence of discontinuities within a jointed rock mass, which can be key with respect to modelling fluid migration and fault slip. Discontinuum methods (e.g., DEM) can more accurately incorporate the influence of a discontinuity network in the model, but is limited in how well it can model crack growth. A recent development in discontinuum modelling are the use of lattice and bonded particle models to more accurately simulate crack growth (e.g., Bakhshi et al., 2018; Pierce et al., 2007; Xing et al., 2018), and amongst these is the 3-D hybrid lattice and bonded-particle based model XSite^{TM} developed by Itasca (Damjanac et al., 2016). The XSite^{TM} software (Itasca Consulting Group Inc, 2013) is a special-purpose numerical code developed for simulating fluid injection and hydraulic fracturing within a discontinuous domain (Bakhshi et al., 2018; Xing et al., 2018). In this study XSite^{TM} modelling was performed. Different stress regimes were imposed as boundary conditions for which fluid injection was simulated in proximity to a critically oriented fault. The size of the fault spans 1 km which allows for a maximum event of approximately M4 (e.g., Zoback & Gorelick, 2012), which is similar to larger events detected in association with injection-induced seismicity. The model properties are taken from those back-analyzed for the Montney by Mckean (2017), including: ρ = 2600 kg/m^3, E = 42 GPa, fracture toughness = 2.3 MPa·m$^{0.5}$ and permeability = 10^{-20} m^2. The friction angle assumed for the fault was 31°. The vertical stress is selected to correspond with a depth of 1850 m for each of the three scenarios, with the two horizontal stresses being selected based on the stress regime being modelled. The injection rate and time were kept constant for all scenarios (see Figure 4 a, b, and c).

The 'b-values' as well as the seismogenic index, Σ, (Shapiro et al., 2010) was calculated based on the simulated microseismic data from the numerical models. The results are shown in Figure 5 and the overall measured parameters are summarized in Table 2. These show that the built-in calculation of microseismicty in XSite™ can reproduce the empirically derived correlations of b-value and stress regime (i.e. $b_{NR}>b_{SS}>b_{TH}$). Moreover, the results reveal the correlation between the large magnitude events (LME) as well as the total number of events for each stress regime (i.e. NR<SS<TH), confirming that the potential for larger magnitude earthquakes is greater for thrust faulting regimes. The value of Σ (Table 2) was found to be almost the same in each simulation; thus, it could not be used as a marker for the analysis of stress regime and risk of induced seismicity in the same formation. It appears to be independent of the stress regime.

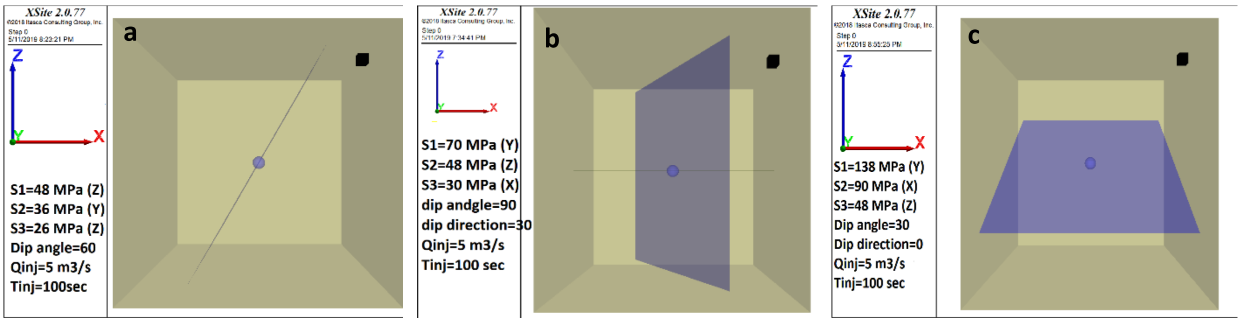

Figure 4 – XSite^{TM} model geometries showing the stress boundary conditions and fault dip for the following fault/stress regimes: a) Normal (NR), b) Strike-slip (SS), c) Thrust (TH)

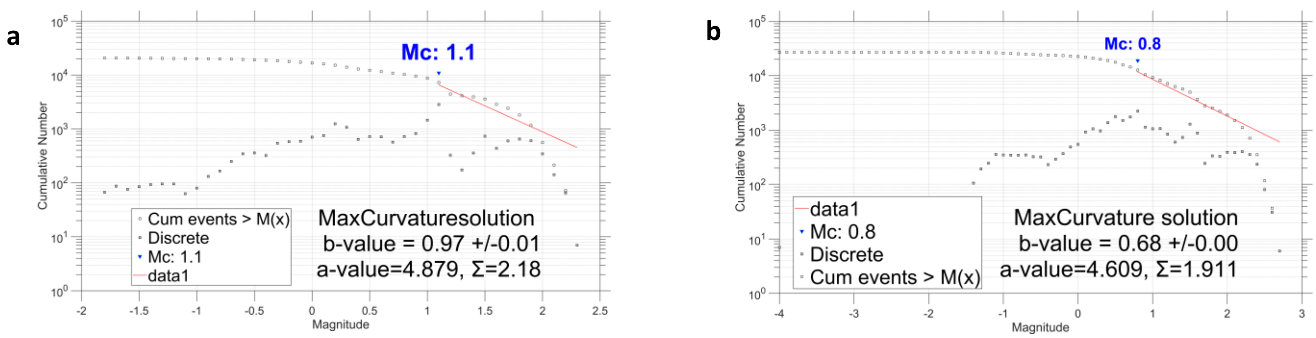

Figure 5 - The magnitude-frequency distribution calculated by the XSite^{TM} models for the: a) strike-slip and b) thrust fault stress regimes

Table 2 – Summary of XSite^{TM} modelling results

Stress regime	$S_1 - S_3$ [MPa] (MPa/km)	$\frac{S_1}{S_3}$	b-value	Σ	LME	# of Events
Normal	22 (11.25)	1.85	1.00±0.01	1.914	1.9724	20314
Strike-slip	40 (20)	2.33	0.97±0.01	2.18	2.3378	20765
Thrust	90 (45)	2.875	0.68±0.00	1.911	2.7499	29638

Acknowledgements

The support and assistance of the Itasca Consulting Group and the Natural Sciences and Engineering Research Council of Canada (NSERC) are deeply appreciated.

References

Aki, K. (1965). Maximum likelihood estimate of b in the formula logN=a-bM and its confidence limits. Bulletin of the Earthquake Research Institute.

Amini, A., & Eberhardt. (2017). An Investigation on the Effects of Different Stress Regimes on the Magnitude Distribution of Induced Seismic Events. In *Geoconvention*. Calgary.

Bakhshi, E., Rasouli, V., Ghorbani, A., Fatehi Marji, M., Damjanac, B., & Wan, X. (2018). Lattice Numerical Simulations of Lab-Scale Hydraulic Fracture and Natural Interface Interaction. *Rock Mechanics and Rock Engineering*. https://doi.org/10.1007/s00603-018-1671-2

Bunger, A., McLennan, J., & Jeffrey, R. (2013). *Effective and sustainable hydraulic fracturing*.

Cipolla, C., Warpinski, N., & Exhibition, M. M. (2008). Hydraulic fracture complexity: diagnosis, remediation, and explotation. In *In SPE Asia Pacific Oil and Gas Conference and Exhibition*. Society of Petroleum Engineers.

Damjanac, B., Detournay, C., & Cundall, P. A. (2016). Application of particle and lattice codes to simulation of hydraulic fracturing. *Computational Particle Mechanics*, *3*(2), 249–261. https://doi.org/10.1007/s40571-015-0085-0

Goebel, T. H. W., Kwiatek, G., Becker, T. W., Brodsky, E. E., & Dresen, G. (2017). What allows seismic events to grow big?: Insights from b-value and fault roughness analysis in laboratory stick-slip experiments. *Geology*, *45*(9), 815–818. https://doi.org/10.1130/G39147.1

Gutenberg, B., & Richter, C. F. (1944). FREQUENCY OF EARTHQUAKES IN CALIFORNIA*. *Bulletin of the Seismological Society of America*, (34), 185–188. Retrieved from https://pubs.geoscienceworld.org/ssa/bssa/article-pdf/34/4/185/2690674/BSSA0340040185.pdf

Healy, J., Rubey, W., Griggs, D., & CB Raleigh. (1968). The denver earthquakes. *Science*. Retrieved from https://earthquake.usgs.gov/static/lfs/research/induced/Healy-et-al-1968-Science-(New-York-NY).pdf

Itasca Consulting Group Inc. (2013). *HF simulator, version 1.9, user's guide*. Itasca Consulting Group Inc.

Maxwell, S. C. (2013). Anomalous induced seismic deformation associated with hydraulic fracturing. *Society of Petroleum Engineers - SPE Canadian Unconventional Resources Conference 2013 - Unconventional Becoming Conventional: Lessons Learned and New Innovations*, *1*, 727–738. Retrieved from https://www.engineeringvillage.com/share/document.url?mid=cpx_52c24f28145700c9863M56f410178163125&database=cpx

Mckean, S. H. (2017). *Geomechanical Properties of the Montney and Sulphur Mountain Formations.* University of Calgary. http://hdl.handle.net/11023/4103

Pierce, M., Cundall, P., & Potyondy, D. (2007). A synthetic rock mass model for jointed rock. In *In Proceedings of the first CA–US rock mechanics symposium* (pp. 341–349). Vancouver, BC. Retrieved from https://books.google.com/books?hl=en&lr=&id=9N_qBgAAQBAJ&oi=fnd&pg=PA341&dq=synthetic+rock+mass+model+for+jointed+rocks&ots=uvNMlq4OlS&sig=MU4iQTFlzRMDEfeIHGKaoN0rW7I

Rutqvist, J., Rinaldi, A. P., Cappa, F., & Moridis, G. J. (2013). Modeling of fault reactivation and induced seismicity during hydraulic fracturing of shale-gas reservoirs. *Journal of Petroleum Science and Engineering*, *107*, 31–44. https://doi.org/10.1016/J.PETROL.2013.04.023

Scholz, C. H. (2015). On the stress dependence of the earthquake *b* value. *Geophysical Research Letters*, *42*(5), 1399–1402. https://doi.org/10.1002/2014GL062863

Schorlemmer, D., Wiemer, S., & Wyss, M. (2005). Variations in earthquake-size distribution across different stress regimes. *Nature*, *437*(7058), 539–542. https://doi.org/10.1038/nature04094

Shapiro, S. A., Dinske, C., Langenbruch, C., & Wenzel, F. (2010). Seismogenic index and magnitude probability of earthquakes induced during reservoir fluid stimulations. *The Leading Edge*, *29*(3), 304–309. https://doi.org/10.1190/1.3353727

Utsu, T. (1965). A method for determining the value of b in a formula log n = a – bM showing the magnitude-frequency relation for earthquakes. *Geophys. Bull. Hokkaido Univ.*, *13*, 99–103.

Wiemer, S., & Wyss, M. (2000). Minimum magnitude of completeness in earthquake catalogs: Examples from Alaska, the Western United States, and Japan. *Bulletin of the Seismological Society of America*, *90*(4), 859–869. https://doi.org/10.1785/0119990114

Xing, P., Yoshioka, K., Adachi, J., El-Fayoumi, A., Damjanac, B., & Bunger, A. P. (2018). Lattice simulation of laboratory hydraulic fracture containment in layered reservoirs. *Computers and Geotechnics*, *100*, 62–75. https://doi.org/10.1016/J.COMPGEO.2018.03.010

Zoback, M. D., & Gorelick, S. M. (2012). Earthquake triggering and large-scale geologic storage of carbon dioxide. *Proceedings of the National Academy of Sciences of the United States of America*, *109*(26), 10164–10168. https://doi.org/10.1073/pnas.1202473109